Journal of
Materials Chemistry B

Accepted Manuscript

ROYAL SOCIETY OF CHEMISTRY

www.rsc.org/materialsB

Journal Name

COMMUNICATION

A facile and one-step ethanol-thermal synthesis of MoS_2 quantum dots for two-photon fluorescence imaging

Received 00th January 20xx,
Accepted 00th January 20xx

DOI: 10.1039/x0xx00000x

www.rsc.org/

Wei Gu,[a] Yinghan Yan,[a] Xuni Cao,[b] Cuiling Zhang,[*a] Caiping Ding[a] and Yuezhong Xian[*a]

Two-photon fluorescenct (TPF) molybdenum disulfide quantum dots (MoS_2 QDs) were synthesized through a facile and one-step solvothermal approach. The MoS_2 QDs exhibit small size and high stability. Because of low toxicity and TPF ability, the MoS_2 QDs are successfully applied in the two-photon fluorescence bio-image.

INTRODUCTION

With the development of two-photon microscopy, two-photon fluorescence imaging has become a powerful tool for research in biological areas because of its unique advantages, such as low tissue autofluorescence, large penetration depth, reduced photobleaching and so on.[1-4] Fluorescence probes with two-photon excitation have been widely applied in TPF imaging,[5, 6] and which can simultaneously absorb two less-energetic photons to reach the excited state of fluorophores. The TPF probes for cellular imaging should possess large two-photon absorption cross section, low toxicity and low photobleaching. Nowadays, great successes have been made on the synthesis of TPF probes, including organic dyes, semiconductor quantum dots, rare earth ions doped nanoparticles and carbon-based materials (carbon dots and graphene quantum dots (GQDs)). However, the poor photobleaching and little two-photon absorption cross section of organic dyes[7] and unavoidable toxicity of heavy metal of semiconductor quantum dots[8] overwhelmingly limit their positive applications for cellular imaging. Although carbon dots and GQDs do not exist these problems, and have been extensively used as TPF probes,[9, 10] searching for stable and non-toxic alternatives obtained by a facile synthesis route is still an intense challenge.

Recently, as a kind of typical layered transition-metal dichalcogenide, molybdenum disulfide (MoS_2) has drawn great attention, for it can be easily exfoliated from molybdenite compound. The crystal structure is consisting of covalently bonded S-Mo-S single layers interacting by Van der Waals forces.[11, 12] Compared with MoS_2 nanosheets, MoS_2 QDs have stronger quantum confinement and edge effects, which will make them show unique and extra electrical/optical properties. So far, MoS_2 QDs have been used in fluorescent sensor,[13] hydrogen evolution reaction[14] and bioimaging.[15] General methods for the synthesis of MoS_2 QDs can be classified into two types: bottom-up and top-down. For the former, MoS_2 QDs were synthesized through the hydrothermal route by using molybdate salt and thiol-containing small molecules as precursors.[13, 16] The final product was obtained by the time-consuming dialysis process. For the latter, MoS_2 QDs were prepared by a variety of methods, such as mechanical and chemical exfoliation,[14, 17-19] electrochemically induced Fenton reaction,[20] thermal ablation method[21] and so on. For instance, Shaijumon's group reported to prepare MoS_2 QDs using a liquid exfoliation technique involving bath sonication followed by ultrasound probe sonication of MoS_2 flakes.[14] Li and co-workers demonstrated that electrochemically induced Fenton reaction could be used to generate QDs by etching MoS_2 nanosheets.[20] Recently, Wu et al. prepared MoS_2 QDs though thermal ablation of MoS_2 nanosheets in N, N-dimethylformamide (DMF) which has a high boiling point.[21] Despite the great success with the synthesis of MoS_2 QDs, it is urgently to develop a simple approach for the preparation of MoS_2 QDs with stable fluorescence.

[a] *Department of Chemistry, School of Chemistry and Molecular Engineering, East China Normal University, 500 Dongchan Road, Shanghai 200241, China. Email: clzhang@chem.ecnu.edu.cn; yzxian@chem.ecnu.edu,cn.*
[b] *School of Biotechnology, East China University of Science and Technology, 130 Meilong Road, Shanghai 200237 (China)*

† Electronic Supplementary Information (ESI) available: Experimental section, Raman spectrum, XPS spectra, pH-depended fluorescence spectrum, Hoechst 33342/PI staining, TPF images of MDA-MB-468 incubated for different time, TPF images of MDA-MB-468 and Hela cells , fluorescence spectrum of MoS_2 QDs in presence of DNA, control experiment for TPF imaging, photostability of MoS_2 QDs within cells. See
DOI: 10.1039/x0xx00000x

Herein, we report the design and synthesis of MoS_2 QDs for TPF cellular imaging. The MoS_2 QDs were prepared by a facile, environmental-friendly, top-down, ethanol-thermal route from bulk MoS_2. These QDs exhibit stable TPF, high dispersibility, small size, non-toxicity and good biocompatibility. Furthermore, TPF imaging for cellular nucleus is successfully realized using MoS_2 QDs as probe. We believe the MoS_2 QDs are the kind of promising probe for the applications in vitro and vivo TPF bio-imaging.

RESULTS AND DISCUSSION

MoS_2 QDs were prepared by the combination of the ultrasonication and ethanol-thermal treatment. The as-prepared MoS_2 QDs exhibit bright blue fluorescence. Uniform MoS_2 QDs without aggregation are observed from the TEM image (Fig. 1a). The lateral size distribution of MoS_2 QDs ranged from 1.2 to 4.2 nm, and the average size is about 2.9 nm. The suitable size distribution ensures them with the possibility to enter the cellular nucleus. Because of the low boiling point of ethanol, the as-prepared MoS_2 QDs do not agglomerate after removing the solvent by vacuum distillation and re-dispersing in water. The highly crystalline structure of the QDs with hexagonal lattice are visualized on the high-resolution TEM (HRTEM) image (Fig. 1b) and the lattice fringe spacing is 0.27 nm deriving from the (100) lattice of MoS2.[22, 23] As shown in Fig. 1c, the thickness of MoS_2 QDs varies from 1.4 to 2.8 nm, which is comparable with the interlayer space of few-layer MoS_2 nanosheets.[24, 25]

XRD pattern of MoS_2 QDs is then investigated, and the bulk MoS_2 is used as a reference. It shows a strong diffraction peak at 2θ= 14.41° and three lower peaks at 2θ=32.71°, 39.56°, and 49.82° for bulk MoS_2 (Fig. 1d, red line).These peaks were attributed to the (002), (100), (103) and (105) planes of MoS_2, respectively. For MoS_2 QDs (Fig. 1d, black line), only two peaks can be detected at 2θ=14.37° (002), 39.57° (103), and the signal of the (002) obviously decreased with the disappearance of most of other peaks, indicating the formation of mono-or few-layered MoS_2 QDs. Besides, Raman spectra of MoS_2 QDs exhibited two typical phonon modes of in-plane vibration of Mo and S atoms (E^1_{2g}) and out-of-plane vibration of S atoms (A_{1g}) at 379.2 cm^{-1} and 403.9 cm^{-1}, with a frequency difference of 24.3 cm^{-1} (Fig. S1).[6, 26] According to the "frequency difference-thickness relation" of exfoliated MoS_2 nanosheets, the frequency difference could be corresponded to that of few-layered MoS_2 QDs,[24] which is consistent with the AFM measurement. To explore the changes of chemical composition, XPS of the QDs is characterized. As shown in Fig. S2a and S2b, Mo 3d3/2, Mo 3d5/2, S 2s, S 2p1/2, S 2p3/2 peaks are observed at 232.9, 229.7, 226.9, 163.8, 162.6 eV, which belong to the dominant 2H MoS_2 phase of the as-prepared MoS_2 QDs.[27, 28] The characteristic peaks arising from Mo 3d3/2, Mo 3d5/2 corresponded to the +4 oxidation of Mo, and the S 2p3/2 at 162.6 eV ascribed to the -2 oxidation state of S.[29] Low intensity peak at 236.0 eV may result from slight oxidation of Mo during solvothermal reaction. These results demonstrate that the MoS_2 QDs are successfully prepared.

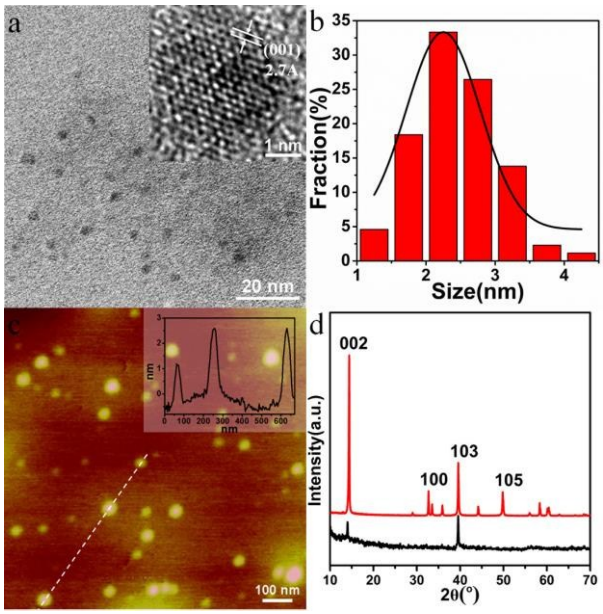

Fig. 1 (a) TEM, (b) HRTEM, and (c) AFM images of MoS_2 QDs, (d) the XRD patterns of MoS_2 QDs (black) and bulk MoS_2 (red). The inset in (a) and (c) shows the lateral size distribution and the height profile along the line overlaid on the image.

UV-vis spectrum of the MoS_2 QDs shows a shoulder peak at about 277 nm (black line in Fig. 2a), which could be attributed to blue-shifted convoluted Z, C, and D excitonic peaks.[23, 30] Under the irradiation of 365 nm, MoS_2 QDs solution displays a strong blue fluorescence (blue line in Fig. 2a and inset in the Fig. 2a). Fig. 2b exhibits the fluorescence emission spectra of MoS_2 QDs at excitation wavelengths ranging from 300 to 380 nm. It can be seen that the emission peak shows a red-shift (from ca. 400 nm to 460 nm) as the excitation shifts towards longer wave wavelengths. The excitation-dependent fluorescence property has been widely reported, such as GQDs[31], carbon dots[32], MoS_2 QDs[20, 21], and so on. Although the exact origin of excitation-dependent photoluminescence of

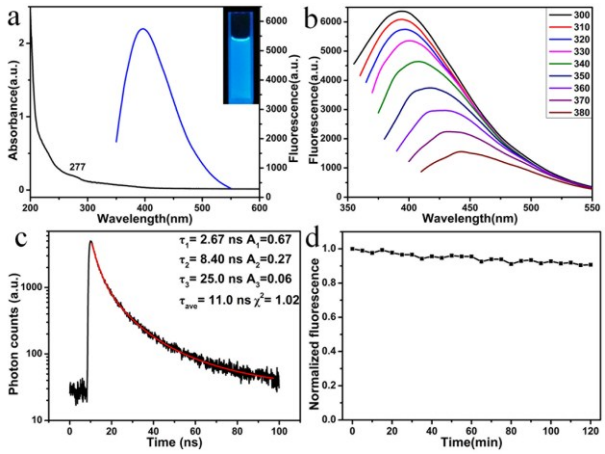

Fig. 2 (a) UV-vis spectrum (black) and fluorescence spectrum (blue) of MoS_2 QDs (inset: photograph of MoS_2 QDs under irradiation of 365 nm), (b) emission spectra of MoS_2 QDs at different excitation wavelengths ranging from 300 to 380 nm, (c) fluorescence lifetime of MoS_2 QDs by monitoring the emission at 410 nm (Ex: 340 nm), (d) photostability of MoS_2 QDs under excitation of 345 nm.

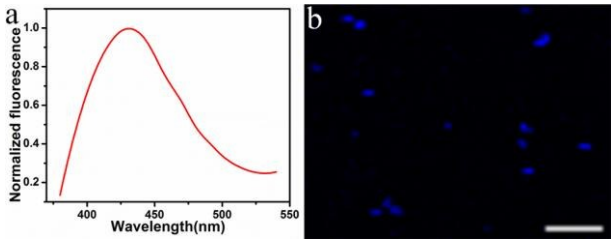

Fig. 3 (a) Two-photon fluorescence of the MoS_2 QDs (Ex: 690 nm), (b) TPF image of solid MoS_2 QDs (Ex: 690 nm, scale bar: 5 μm).

these QDs are still under debate, it might be attribute to the polydispersity or the surface state of MoS_2 QDs[33]. The fluorescence intensity decreases remarkably with the increase of the excitation wavelengths, which is consistent with MoS_2 QDs or fluorescent MoS_2 nanoflakes prepared by other methods.[13, 20, 34] In addition, the fluorescence quantum yield was measured using quinine sulfate as the standard, and it was about 3.1%, which was comparable to those of the reported MoS_2 QDs and GQDs.[13, 35, 36] The fluorescence lifetime of MoS_2 (Fig. 2c) was τ_{ave}= 11.0 ns, suggesting that the MoS_2 QDs were suitable for biological and optoelectronic applications.[37]

The stability of fluorophores is crucially important for bioimaging application. Significantly, the MoS_2 QDs display excellent photostability. The QDs retain almost the original fluorescence intensity after irradiation for 2 h (Fig. 2d). The effect of pH on the performances of QDs was further investigated. As shown in Fig. S3a, the as-prepared MoS_2 QDs exhibit higher fluorescence intensity under acidic condition than that of alkaline condition. As the pH was switched repeatedly between 2 and 12, the fluorescence intensity could be varied reversibly (Fig. S3b). Compared with the conventional semiconductor quantum dots, the results indicate that the pH hardly affects the fluorescence properties of the MoS_2 QDs.

The TPF properties of the MoS_2 QDs were further evaluated. As shown in Fig. 3a, the as-prepared MoS_2 QDs show the maximum TPF emission at 428 nm with the excitation wavelength at 690 nm. From TPF imaging of MoS_2 QDs (Fig. 3b), it can be seen that MoS_2 QDs display blue fluorescence under excitation of 690 nm. Recently, Song's group reported synthesis of water-soluble monolayer MoS_2 QDs through bottom-up route with N-acetyl-L-cysteine (NAC) as capping reagent[16], and the QDs show upconversion fluorescence due to the two successive energy transfer from capping reagent NAC to MoS_2 QDs accompanied with the depletion of intermediate excited state by the upconversion process. With regard to our strategy, MoS_2 QDs were obtained through a top-down route without surface ligand, therefore, the TPF mechanism might be that two photons arrive QDs simultaneously and combine their energies to promote MoS_2 in ground states to an excited states, and then proceed along the normal fluorescence-emission pathway. As it has been well-recognized, the two-photon action cross section is an essential attribute for two-photon excited materials. By using rhodamine B as the reference, the two-photon absorption cross-section of MoS_2 QDs is estimated to be 9500±500 GM (Goeppert-Mayer unit, with 1 GM = 10^{-50} cm^4s/photon), which is much larger than that of the organic dyes and compatible to that of semiconductor quantum dots and graphitic-C_3N_4 quantum dots[38, 39].

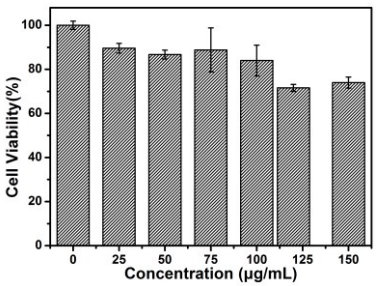

Fig. 4 Cell viability by MTT assay of MDA-MB-468 Cells. (The concentrations of MoS_2 QDs are 0, 25, 50, 75, 100, 120, 150 μg/mL, respectively)

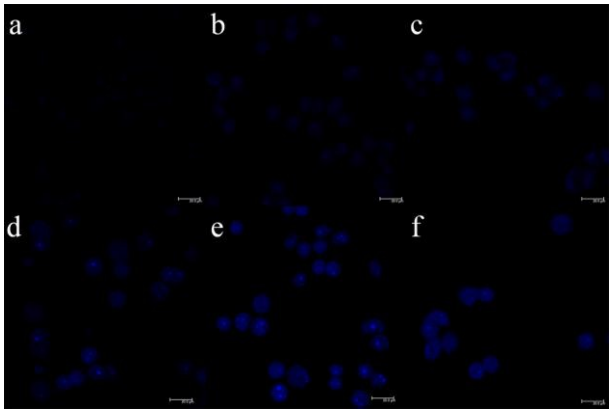

Fig. 5 TPF images of MDA-MB-468 cells incubated with MoS_2 QDs (50 μg/mL) for 0 min to 3 h. (a: 0 min, b: 10 min, c: 30 min, d: 1 h, e: 2 h, f: 3h)

Toxicity assessment is also critical importance for the biological application. In this work, MTT assay was used to evaluate the cytotoxicity of MoS_2 QDs using MDA-MB-468 cells as model. As shown in Fig. 4, low concentrations of MoS_2 QDs are little toxic for these cells. Moreover, the cells maintained about 80% viability after incubated with QDs as high as 150 μg/mL. In addition, the cells incubated with different concentrations of MoS_2 QDs were stained with Hoechst 33342 and PI (Fig. S4). It is well known that Hoechst 33342 can penetrate the cell membranes and label the cell nucleus with blue fluorescence, while PI is commonly used for identifying dead cells. It can be seen that the cell viability is very well even the concentration of MoS_2 QDs is up to 150 μg/mL. Almost no dead cells are found because the living cells can't be stained by PI. These data indicate that the MoS_2 QDs might be promising probe in cellular imaging.

To demonstrate the MoS_2 QDs utility for TPF bioimaging, we further employ QDs for in vitro cell imaging. Fig. 5 and Fig. S5 show the TPF images of MDA-MB-468 cells incubated with MoS_2 QDs for different time. It can be observed that weak fluorescence appears in the cells within 10 min. The

fluorescence intensity is enhanced gradually with incubation time, and maintains a constant intensity after 2 h. To confirm the distribution of MoS_2 QDs in the cells, the TPF images were further investigated by culturing MDA-MB-468 and Hela cells with QDs (50 μg/mL) for 2 h. It can be observed in Fig. S6 that MoS_2 QDs are able to label the cell nucleus of MDA-MB-468 cells and Hela cells, which is similar with that of graphitic-C_3N_4 QDs reported by Xie et al.[39]. There may be some specific interactions between MoS_2 QDs and DNA (main components of chromatin). As shown in Fig. S7, with the addition of DNA, the fluorescence intensity of the solution of MoS_2 QDs increases. Although the mechanism is not clear, it might be associated with its charge-transfer excited states that are sensitive to external environment. Liu et al reported a water-soluble nanodot with an average diameter of 3.3 ± 0.5 nm for TPF imaging of cellular nucleus[40]. They find the enhanced fluorescence with the addition of DNA, and ascribe the phenomenon to the significant increment hydrophobicity of nanodots with interaction with DNA. As a control, scarcely any fluorescence could be found in the cells without the MoS_2 QDs (Fig. S8). What's more, the fluorescence intensity of the MoS2 QDs within cells almost keeps unchanged after irradiation under 690 nm for 2 h (Fig. S9). The results imply that the QDs have the great potential in applications of the TPF bioimaging.

CONCLUSIONS

In summary, a facile, top-down, one-step ethanol-thermal route has been developed to synthesize MoS_2 QDs with TPF behaviour. The QDs exhibit small size, high dispersibility, low cytotoxicity and excellent photostability. Most importantly, the as-prepared MoS_2 QDs are well suitable for staining cellular nucleus, which are more adaptable for the further study of TPF bioimaging. Such MoS_2 QDs are promising probes for the applications of biological and deep-tissue imaging.

ACKNOWLEDGEMENTS

We acknowledge financial support from the National Natural Science Foundation of China (21175046) and the Shanghai Natural Science Foundation (15ZR1411600).

Notes and references

1 W. Denk, J. H. Strickler and W. W. Webb, *Science*, 1990, **248**, 73-76.
2 F. Helmchen and W. Denk, *Nat. Methods*, 2005, **2**, 932-940.
3 H. Kim, B. R. Kim, J. H. Hong, J.-S. Park, K. J. Lee and B. R. Cho, *Angew. Chem. Int. Ed.*, 2007, **46**, 7445-7448.
4 H. J. Kim, J. H. Han, M. K. Kim, C. S. Lim, H. Kim and B. R. Cho, *Angew. Chem. Int. Ed.*, 2010, **49**, 6786-6789.
5 L. Cao, X. Wang, M. J. Meziani, F. Lu, H. Wang, P. G. Luo, Y. Lin, B. A. Harruff, L. M. Veca, D. Murray, S.-Y. Xie and Y.-P. Sun, *J. Am. Chem. Soc.*, 2009, **129**, 11318-11319.
6 S. Balendhran, J. Z. Ou, M. Bhaskaran, S. Sriram, S. Ippolito, Z. Vasic, E. Kats, S. Bhargava, S. Zhuiykovd and K. Kalantar-zadeh, *Nanoscale*, 2012, **4**, 461-466.
7 C. Xu and W. W. Webb, *J. Opt. Soc. Am. B*, 1996, **13**, 481-491.
8 K. B. Male, B. Lachance, S. Hrapovic, G. Sunahara and J. H. T. Luong, *Anal. Chem.*, 2008, **80**, 5487-5493.
9 B. Kong, A. Zhu, C. Ding, X. Zhao, B. Li and Y. Tian, *Adv. Mater.*, 2012, **24**, 5844-5848.
10 Q. Liu, B. Guo, Z. Rao, B. Zhang and J. R. Gong, *Nano Lett.*, 2013, **13**, 2436-2441.
11 A. Molina-Sánchez and L. Wirtz, *Phys. Rev. B*, 2011, **84**, 1-8.
12 M. Chhowalla, H. S. Shin, G. Eda, L.-J. L. , K. P. Loh and H. Zhang, *Nat. Chem.*, 2013, **5**, 263-275.
13 Y. Wang and Y. Ni, *Anal. Chem.*, 2014, **86**, 7463-7470.
14 D. Gopalakrishnan, D. Damien and M. M. Shaijumon, *ACS nano*, 2014, **8**, 5297-5303.
15 J. Ou, A. F. Chrimes, Y. Wang, S. Tang, M. S. Strano and K. Kalantar-zadeh, *Nano Lett.*, 2014, **14**, 857-863.
16 H. Huang, C. Du, H. Shi, X. Feng, J. Li, Y. Tan and W. Song, *Part. Part. Syst. Char.*, 2015, **32**, 72-79.
17 G. Eda, H. Yamaguchi, D. Voiry, T. Fujita, M. Chen and M. Chhowalla, *Nano Lett.*, 2011, **11**, 5111-5116.
18 H. D. Ha, D. J. Han, J. S. Choi, M. Park and T. S. Seo, *Small*, 2014, **10**, 3858-3862.
19 X. Zhang, Z. Lai, Z. Liu, C. Tan, Y. Huang, B. Li, M. Zhao, L. Xie, W. Huang and H. Zhang, *Angew. Chem. Int. Edit.*, 2015, **54**, 1-5.
20 B. Li, L. Chen, H. Zou, J. Lei, H. Luo and N. Li, *Nanoscale*, 2014, **6**, 9831-9838.
21 S. Xu, D. Li and P. Wu, *Adv. Funct. Mater.*, 2015, 25, 1127-1136.
22 Y. Liu, H. Nan, XingWu, W. Pan, W. Wang, J. Bai, W. Zhao, L. Sun, X. Wang and Z. Ni, *ACS nano*, 2013, **7**, 4202-4209.
23 Y. C. Wang, J. Z. Ou, S. Balendhran, A. F. Chrimes, M. Mortazavi, D. D. Yao, M. R. Field, K. Latham, V. Bansal, J. R. Friend, S. Zhuiykov, N. V. Medhekar, M. S. Strano and K. Kalantar-zadeh, *ACS nano*, 2013, **7**, 10083-10093.
24 L. Changgu, Y. Hugen, L. E. Brus, T. F. Heinz, J. Hone and S. Ryu, *ACS nano*, 2010, **4**, 2695-2700.
25 Q. Ji, Y. Zhang, T. Gao, Y. Zhang, D. Ma, M. Liu, Y. Chen, X. Qiao, P.-H. Tan, M. Kan, J. Feng, Q. Sun and Z. Liu, *Nano Lett.*, 2013, **13**, 3870-3877.
26 H. Li, Q. Zhang, C. C. R. Yap, B. K. Tay, T. H. T. Edwin, A. Olivier and D. Baillargeat, *Adv. Funct. Mater.*, 2012, **22**, 1385-1390.
27 N. H. Turner and A. M. Single, *Surf. Interface Anal.*, 1990, **15**, 215-222.
28 V. O. Koroteev, L. G. Bulusheva, I. P. Asanov, E. V. Shlyakhova, D. V. Vyalikh and A. V. Okotrub, *J. Phys. Chem. C*, 2011, **115**, 21199-21204.
29 J. Xie, J. Zhang, S. Li, F. Grote, X. Zhang, H. Zhang, R. Wang, Y. Lei, B. Pan and Y. Xie, *J. Am. Chem. Soc.*, 2013, **135**, 17881-17888.
30 J. Wilcoxon and G. Samara, *Phys. Rev. B*, 1995, **51**, 7299-7302.
31 Y. Li, Y. Hu, Y. Zhao, G. Shi, L. Deng, Y. Hou and L. Qu, *Adv. Mater.,* 2011, **23**, 776-780.
32 H. Nie, M. Li, Q. Li, S. Liang, Y. Tan, L. Sheng, W. Shi and S. X.-A. Zhang, *Chem. Mater.*, 2014, **26**, 3104-3112.
33 D. Gopalakrishnan, D. Damien, B. Li, H. Gullappalli, V. K. Pillai, P. M. Ajayan and M. M. Shaijumon, *Chem. Comm.*, 2015, **51**, 6293-6296.
34 V. Stengl and J. Henych, *Nanoscale*, 2013, **5**, 3387-3394.
35 R. Liu, D. Wu, X. Feng and K. Mullen, *J. Am. Chem. Soc.*, 2011, **133**, 15221-15223.
36 D. Wang, L. Wang, X. Dong, Z. Shi and J. Jin, *Carbon*, 2012, **50**, 2147-2154.
37 J. Peng, W. Gao, B. K. Gupta, Z. Liu, R. Romero-Aburto, L. Ge, L. Song, L. B. Alemany, X. Zhan, G. Gao, S. A. Vithayathil, B. A. Kaipparettu, A. A. Marti, T. Hayashi, J. Zhu and P. M. Ajayan, *Nano Lett.*, 2012, **12**, 844-849.
38 U. Resch-Genger, M. Grabolle, S. Cavaliere-Jaricot, R. Nitschke and T. Nann, *Nat. Methods*, 2008, **5**, 763-775.
39 X. Zhang, H. Wang, H. Wang, Q. Zhang, J. Xie, Y. Tian, J. Wang and Y. Xie, *Adv. Mater.*, 2014, **26**, 4438-4443.

40 K. Y. Pu, K. Li, X. Zhang and B. Liu, *Adv. Mater.*, 2010, **22**, 4186-4189.

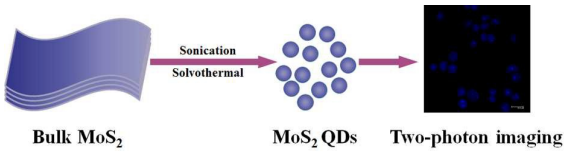

MoS_2 quantum dots with two-photon fluorescent feature are synthesized through a one-step solvothermal approach and successfully used for cellular bioimaging.